Cocrystallization and Phase Segregation in Blends of Two Bacterial Polyesters

Naoko Yoshie,*[1] *Yoshio Inoue*[2]

[1] Institute of Industrial Science, University of Tokyo, Komaba, Meguro-ku, Tokyo 153-8505, Japan
E-mail: yoshie@iis.u-tokyo.ac.jp
[2] Department of Biomolecular Engineering, Tokyo Institute of Technology, 4259 Nagatsuta, Midori-ku, Yokohama 226-8501, Japan

Summary: By fractional precipitaion of bacterial copolyesters, it has been strongly suggested that the bacterial PHA copolymer normally has broad and/or multimodal chemical composition distribution (CCD). In this paper, we try to review the works on the blends of two bacterial polyesters in order to accumulate knowledge on the relation between CCD and various properties required for the practical application of bacterial copolymers. Phase structures of the blends of poly(3-hydroxybutyrate) [PHB] and poly(3-hydroxybutyrate-*co*-3-hydroxyvalerate) [PHB-HV] and crystallization kinetics of the blends of PHB-HV and poly(3-hydroxybutyrate-*co*-3-hydroxypropionate) [PHB-HP] are described.

Keywords: bacterial copolyesters; blends; crystallization; phase segregation; phase structure

Introduction

The greater parts of bacterial polyhydroxyalkanoates [PHAs] are copolymers consisting of two or more hydroxyalkanoate units. Usually, we expect copolymers to have a narrow chemical composition distribution (CCD), without careful consideration. However, fractional precipitation of bacterial PHA copolymers has shown results contrary to this expectation. Over 20 bacterial PHA copolymers, which were synthesized from various carbon sources by various organisms, were subjected to fractional precipitation and all of them were fractionated into two or more fractions with different chemical compositions.[1] This fact implies that bacterial PHA copolymers normally have broad and/or multimodal CCD. To our knowledge, no biosynthetic methods for accurate control of CCD in PHA copolymers are known currently.

It is natural to expect that CCD influences various properties of PHA. Actually, for bacterial poly(3-hydroxybutyrate-*co*-3-hydroxyvalerate)s [PHB-HVs] and poly(3-hydroxybutyrate-*co*-3-hydroxypropionate)s [PHB-HPs], the comparison of some

 DOI: 10.1002/masy.200550606

properties between the samples *as biosynthesized* and fractionated was performed. It was shown that some of the *as biosynthesized* samples do not have a melting temperature, T_m, expected from the average chemical composition, indicating crystallization with phase segregation.[2,3] Therefore, we need to obtain information on the relations of CCD phase structure and CCD properties for practical applications of bacterial PHA copolymers.

The effects of CCD on various properties of PHA copolymers can be discussed though the analysis of the blends of fractionated PHAs with different chemical compositions. In this paper, we review our recent studies on the phase structures of the blends of PHB with PHB-HV. Such A/AB binary blends can be regarded as copolymers bearing bimodal CCD. PHB-HV copolymers keep high crystallinity throughout a range of compositions from 0 to 100% HV due to the isomorphous behavior.[4,5] So, PHB/PHB-HV blends are semicrystalline/semicrystalline systems. In melt-miscible blends of two semicrystalline polymers, phase segregation precedes crystallization in a greater or lesser extent. As a result, the blends can potentially form many structures varied on the morphological level to which the component polymers are closely mixed. Actually, the PHB/PHB-HV blends form various crystalline phase structures. We also review the studies on the crystallization kinetics of the blends of PHB-HV with PHB-HP. Because of the similarity of the phase structures between the PHB/PHB-HV blends and the PHB-HV/PHB-HP blends, the analysis of the crystallization mechanism of the former blends is highly suggestive for the mechanism of the latter. The degree of phase segregation during the crystallization was observed *in situ* by FTIR microscopy.

Phase Structures in PHB/PHB-HV Blends

Analysis by differential scanning calorimetry (DSC) and polarized microscopy. The phase structures of PHB/PHB-HV blends were analyzed through the measurement of melting thermograms by DSC and the observations of spherulite growth by polarized microscopy.[6,7] PHB/PHB-HV blends show various patterns in the plots of melting temperature, T_m, and the logarithm of spherulite growth rate, log G, as a function of blend composition (wt % of PHB-HV). Four typical patterns of T_m plots are shown in Figure 1. These patterns correspond to different phase structures of type I, II, III, and V. Type IV will be introduced later.

The patterns of T_m and log G change depending on the HV content of PHB-HV. It is well known that PHB is immiscible with a PHB-HV of high HV content, while it is miscible

with a PHB-HV of low HV content.[6,8-10] Thus, the miscibility between PHB and PHB-HV improves with the decrease of the HV content. One of the four typical phase structures

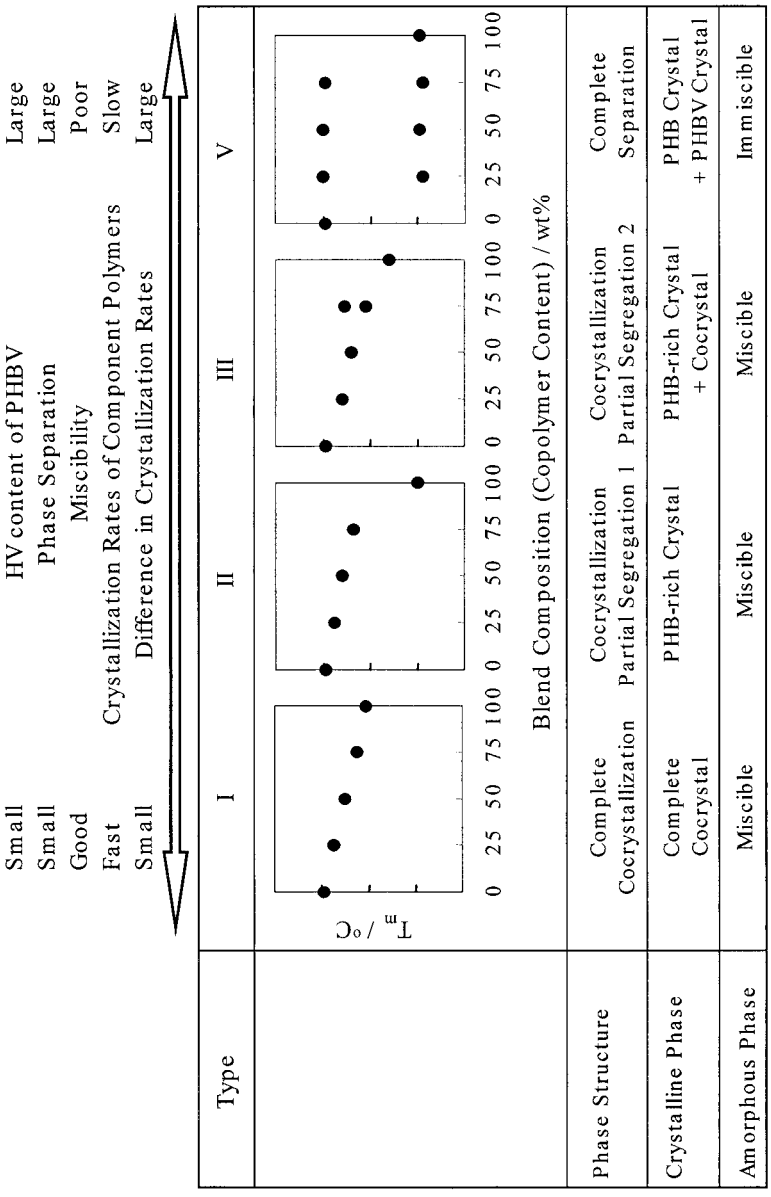

Figure 1. Variation of phase structures in PHB/PHB-HV blends.

(type V) in Figure 1, which is for the blends containing PHB-HV with the highest HV, is for the immiscible blend, and the others (type I-III) are for the miscible ones. When the HV content of PHB-HV is very low (< ca.10 %HV, type I), the plots of T_m and log G against the blend composition of PHB/PHB-HV blends follow a straight line connecting the data for the blend components. As the HV content of PHB-HV becomes a little bit higher (ca. 15-20 %HV, type II), the plots of T_m and log G give a convex curve while they are still located between these of the components. These results indicate that only one crystalline phase is formed in the blends of types I and II. As the HV content further increases (< ca. 20%HV type III), the blends have two melting temperatures. The higher T_m is as high as the T_m of pure PHB while the lower one is positioned between the T_m of PHB and the T_m of PHB-HV. Despite the observation of two melting temperatures, no phase separation was observed by polarized microscopy. The radii of all the spherulites increase linearly with the same rate, which is as high as the G of pure PHB. Thus, two crystalline phases coexist in the same spherulite in the blend of type III. When the HV content of PHB-HV exceeds 30-40 mol%, the blends become immiscible (type V). In this case, polarized microscopy allows us to observe phase separation in the melt state. When the melt is cooled to a crystallization temperature, T_c, spherulites are formed in one of the separated phases and the other phase forms an island of melt in the intraspherulite region. All the spherulites grow at the same rate. When we continue to maintain the T_c, distinct spherulites are formed inside the island of the separated melt. The growth rate of these spherulites cannot be determined because they are small. For this blend, two melting temperatures, which respectively correspond with those of PHB and PHB-HV, are observed. Thus, the separated phases are composed of pure PHB and pure PHB-HV, respectively.

Analysis by ^{13}C CPMAS NMR spectroscopy. The composition in the crystalline phase of the blends forming only one crystalline phase (types I and II) was determined by high-resolution solid-state ^{13}C NMR spectroscopy.[7,11] As mentioned above, PHB-HV is known as a copolymer exhibiting isodimorphism, i.e., the cocrystallization of HB and HV units both in the PHB and PHV crystalline lattices. The composition in the crystalline phase may not necessarily be the same as the HV content of the whole PHB-HV copolymer and actually changes with the crystallization condition.[12,13] The cocrystalline phase of PHB/PHB-HV is, therefore, composed of HB units from PHB, HB units from PHB-HV, and HV units from PHB-HV. The amount of HV units in the cocrystalline phase is not the

same as the product of the PHB-HV content in this phase and the HV content of the whole PHB-HV copolymer. Further, the composition in the crystalline phase probably changes depending on the blend composition and the crystallization condition. Therefore, a complete description of the phase structure of PHB/PHB-HV blends needs both the HV and PHB contents in the crystalline phase.

In a ^{13}C CPMAS NMR spectrum of PHB/PHB-HV, the peaks from PHB completely overlap with those from the HB units of PHB-HV. The determination of the PHB content in the crystalline phase is impossible for normal PHB/PHB-HV blend samples. Therefore, the contrast between PHB and PHB-HV was made by ^{13}C-labeling of the methylene carbons of PHB.[14] Further, when the total HV content in a PHB/PHB-HV blend is small, the peaks from HV units in the ^{13}C CPMAS NMR spectrum are so weak that the estimation of their relative peak area yields a large margin of experimental error. Thus, the methine resonance of HV units was enlarged by ^{13}C labeling for the PHB-HV samples.[14] When we need to explicitly discriminate the PHB [PHB-HV] samples with and without ^{13}C label, we denote them as PHB^E [$PHB\text{-}HV^E$] and PHB^N [$PHB\text{-}HV^N$], respectively.

Figure 2 shows the ^{13}C CPMAS NMR spectra of PHB^E, 50/50 PHB^E/PHB-13%HV^E, and PHB-13%HV^E. In these spectra, the peak area ratios of the main-chain methylene resonance (B2+V2) to the methine resonances of HB (B3) and HV (V3) are obviously different from each other because of the ^{13}C enrichment at B2 (3.4 % ^{13}C) for PHB^E and at V3

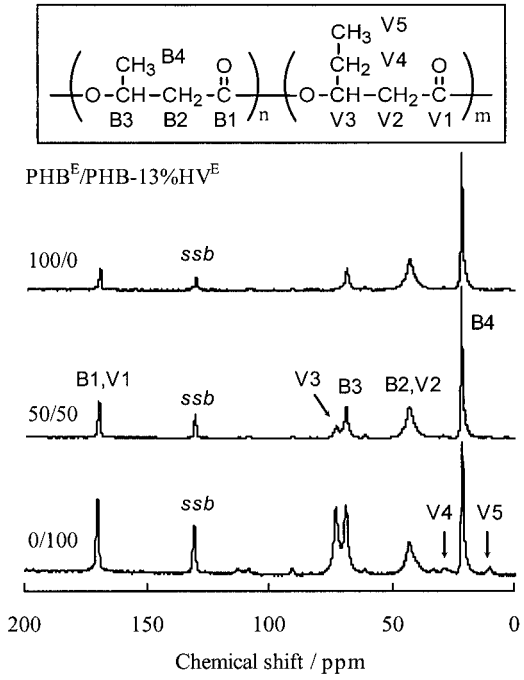

Figure 2. 100MHz ^{13}C CPMAS NMR spectra of PHB^E, 50/50 PHB^E/PHB-13%HV^E, and PHB-13%HV^E. The peaks of spinning side bands are marked with *'ssb'*. Data cited from ref.11 and rearranged.

(12.9 % ^{13}C) for PHB-13%HV^{E}. Since the crystalline phase is emphasized in CPMAS NMR spectra, these peak area ratios reflect the composition in the crystallize phase. The larger peak area ratios of (B2+V2) to B3 and (B2+V2) to V3 for the PHB^{E}/PHB-HV^{E} blend indicate the higher PHB content and the higher HV content in the crystalline phase, respectively. In the actual estimation of the composition in the crystalline phase, the peak ratios of crystalline B2 to crystalline B3 and crystalline B2 to crystalline V3 were determined through the curve decomposition into the crystalline and amorphous peaks by curve fitting software.

In the blends of type I, the PHB content in the crystalline phases, $P_{PHB}{}^{h}$, is similar to the whole composition, which indicates the occurrence of complete cocrystallization. PHB and PHB-HV chains are equally introduced into the crystalline phase without phase segregation; any other mechanism differentiating between PHB and PHB-HV does not work. In the blends of type II, $P_{PHB}{}^{h}$ is unambiguously larger than the whole blend; that is, PHB preferentially enters the crystalline phase.

Crystalline phase structures of PHB/PHB-HV blends. The results for the blends of types I and II indicate the correlation between $P_{PHB}{}^{h}$ and T_m. The melting temperature of the complete cocrystals (type I) lies on a straight line connecting the data for the pure components in the plot of T_m vs. blend composition. On the other hand, the melting temperature of the PHB-rich crystalline phase (type II) has a position higher than the straight line. Thus, the T_m value allows us to presume the composition in the crystalline phase for the blends forming more than one crystalline phase. The higher T_m of the blend of type III is rather close to the melting temperature of pure PHB, indicating the formation of PHB-rich crystals. The lower T_m lies between the melting temperatures of PHB and PHB-HV, indicating the formation of the cocrystals.

As summarized in Figure 1, the PHB/PHB-HV blends form various crystalline phase structures depending on the HV content of PHB-HV. The phase structures are (type I) complete cocrystallization forming crystals whose PHB-HV content is similar to the blend composition, (type II) partial phase segregation (partial cocrystallization) forming PHB-rich crystals, (type III) partial phase segregation (partial cocrystallization) forming PHB-rich crystals and cocrystals, and (type IV) complete separation forming PHB crystals and PHB-HV crystals. In the phase structures of types I-IV, the extent of phase segregation upon the crystallization increases in this order.

Phase structures of miscible PHB/PHB-HV blends crystallized at various temperatures have also been analyzed by DSC and polarized microscopy.[15] The crystalline phase structure of PHB/PHB-HV blends depends on the crystallization temperature though the change is not so large. As T_c increases, the phase segregation proceeds and the PHB-HV content in the crystalline phase decreases.

Crystallization Kinetics in PHB-HV/PHB-HP Blends

***In situ* observation by FTIR microscopy.** The mechanism of phase segregation and cocrystallization was analyzed for PHB-HV/PHB-HP blends through the *in situ* observation of crystallization by FTIR microscopy.[16,17] In order to trace the crystallization process of the blend components separately by a FTIR microscope, deuterated PHB-HV (PHB-HV^D)[18] is blended with normal PHB-HP. The C-D and C=O stretching bands of the IR spectra are used to trace the crystallization of PHB-HV^D and the whole blend, respectively. Five pairs of PHB-HV and PHB-HP were selected so as to make miscible blends with variations in the spherulite growth rates of components and their ratio. The blends show four types of crystalline phase structures. Three of them correspond with types I-III of PHB/PHB-HV blends. The other (type IV) is a complete phase segregation forming PHB-HV crystals and PHB-HP crystals.

The crystallization kinetics of the PHB-HV^D/PHB-HP blends was analyzed through the plot of the relative peak intensities of the C-D and C=O bands as a function of crystallization time. Typical patterns of the plots representing the crystallization of type I-IV are shown in Figure 3. During the crystallization process of the blends of types I and II, the C-D and C=O bands for the blends grow simultaneously. Therefore the formation of only one cocrystalline phase is confirmed. The difference between types I and II is that the growth rate of the bands for type I is just the average rate of the C=O bends for pure PHB-HV^D and pure PHB-HP, while the rate for type II is a little bit higher than the average. In the crystallization process of the blends of types III and IV, the C-D and C=O bands are not in accord with each other, which indicates the formation of two crystalline phases. In the case that the G of PHB-HV^D is higher than that of PHB-HP, the growth rates of the C=O band for pure PHB-HV^D, of the C-D band for the blend, of the C=O band for the blend, and of the C=O band for pure PHB-HP decrease in this order. The difference between the blends of types III and IV is in the growth rate of the C-D band for the blends. The growth rate of the C=O band for the type III blends is lower than that of pure PHB-

HV^D, while the rate for the type IV blends is similar to that of the PHB-HV^D component. Therefore, in the blends of type III, the crystalline phase rich in PHB-HV^D is formed first, which is followed by the formation of crystals containing PHB-HP. On the other hand, the initial crystalline phase in type IV is composed of only PHB-HV^D.

The crystallization mechanism in the blends of PHB-HV and PHB-HP described above is probably applicable to the blends of PHB and PHB-HV. In the following discussion, we consider a blend PHA^H/PHA^L, of which the component PHA^H has higher G than the component PHA^L. It was reported that the crystallization rate[19] and spherulite growth rate[20,21] of PHB-HV is lower than PHB. So, in PHB/PHB-HV blends, PHA^H and PHA^L always represent PHB and PHB-HV, respectively.

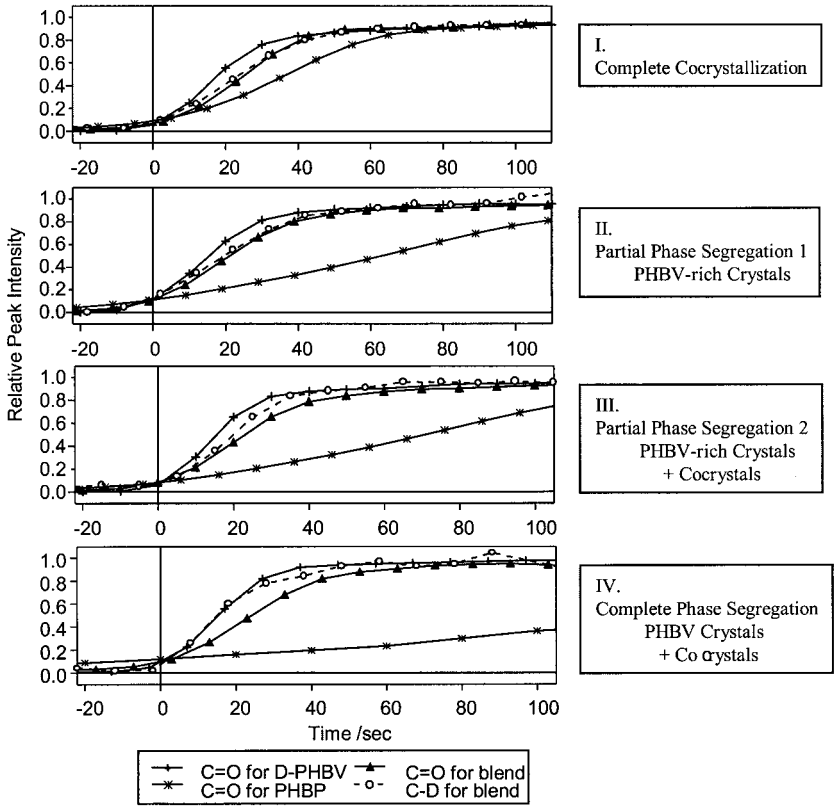

Figure 3. Variation in time dependence of the relative peak intensity for D-PHBV, PHBP and their 1/1 blend. Data cited from ref. 17 and rearranged.

Figure 4 shows a schematic diagram illustrating the crystallization process in the PHA^H/PHA^L blends. PHA^H chains are probably set to crystallize before PHA^L chains are. When PHA^L are intimately mixed with PHA^H and the G of PHA^L is similar to that of PHA^H, the PHA^H chains that are about to crystallize at the growing front of a crystal (or a spherulite) trap those PHA^L-chains in the neighborhood and drag them into the crystalline phase. Any mechanism differenciating PHB-HV from PHB does not works. As a result, the composition in the crystalline phase is the same as the blend composition. The complete cocrystallization [type I] must be explained by this hypothetical process. When the G value of PHA^H becomes lower and/or the G ratio become larger, the PHA^L chains have more chance to escape from the growing front of the crystals and, as a result, a crystalline phase rich in PHA^H is formed. Although the PHA^L content in the PHA^H-rich crystalline phase is still not small, the crystallization event of the blend is finished with the formation of this phase [type II]. When the phase segregation proceeds further and PHA^L content in the PHA^H-rich crystals becomes very small, a substantial amount of PHA^L remains with a small amount of PHA^H in the amorphous phase, which forms separated cocrystals later [type III]. If the phase segregation occurs completely, the crystalline phases of pure PHA^H and the pure PHA^L are formed [type IV].

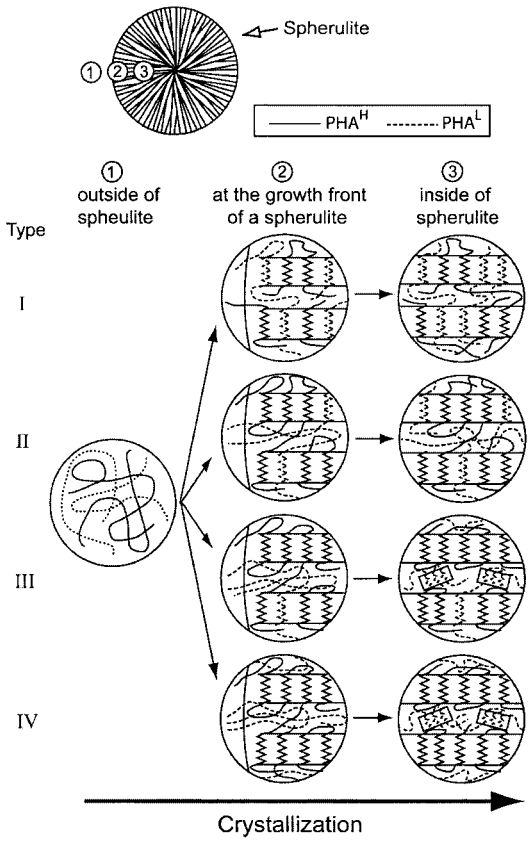

Figure 4. Schematic diagram illustrating the crystallization process in the PHA^H/PHA^L blends. Cited from ref.17 and rearranged.

Therefore, three of the determinant factors for the extent of phase segregation are miscibility, the *G* value of the component polymers, and the *G* ratio of components. The poorer the miscibility, the lower *G*, and the larger *G* ratio favors phase segregation.

Difference in crystalline phase structure between PHBV/PHBP and PHBP/PHBV. The comparison between the PHB-HP/PHB-HV blends (in which PHB-HP has a higher *G* than PHB-HV) and the PHB-HV/PHB-HP blends (in which PHB-HV has a higher *G* than PHB-HP) indicates another factor that affects the crystalline phase structure. The PHB-HP/PHB-HV blends show complete cocrystallization even if the *G* values and their ratio are larger than the values of the PHB-HV/PHB-HP blends showing phase segregation. Therefore, the PHB-HP/PHB-HV blends have a higher tendency for cocrystallization than the PHB-HV/PHB-HP blends.

The difference in the capacity for cocrystallization between PHB-HV/PHB-HP and PHB-HP/PHB-HV is probably related to the difference in the compatibility of HV and HP units to the PHB crystalline lattice. Because of the isomorphous behavior of PHB-HV, PHB-HV showes high crystallinity and forms thick lamellas even at intermediate comonomer composition.[22] In the case of PHB-HV containing less than 20 % HV crystallized at 80-100 °C, the crystallinity exceeds 50 % and the lamella thickness is 5-7 nm,[23,24] which are comparable to the values of the PHB homopolymer. On the other hand, the PHB copolymers other than PHB-HV do not show isomorphous behavior.[25] As a result of the exclusion of comonomer units from the crystalline phase, the crystallinity and lamellar thickness of these copolymers rapidly decrease with the increase of comonomer content. In the case of PHB-HP, the copolymer becomes fully amorphous when the HP content reaches nearly 50 %. Though, to our knowledge, there are no reports on the lamellar thickness of PHB-HP, the thickness of various PHB copolymers showing no isomorphism has been reported[24] and all the copolymers have a similar value. When the comonomer content is 5-10 mol%, the lamellas formed at 80-100 °C have a thickness of 2-3 nm. The lamella thickness of PHBP is probably within this range. Therefore, in the pure state, PHBP forms lamellas which are much thinner than PHBV.

Figure 5 shows a schematic diagram illustrating the difference in the crystallization process between PHB-HV/PHB-HP and PHB-HP/PHB-HV blends. The crystallization in the blends of PHB-HV and PHB-HP is induced by the component having a higher *G*. In PHB-HP/PHB-HV blends, PHB-HP leads the formation of relatively thin lamellas. Any part of the PHB-HV chains easily gets into these lamellas because the HV units in the

chains can participate in the PHB-type crystalline lattice. Therefore, PHB-HV easily cocrystallizes with PHB-HP in PHB-HP/PHB-HV blends. In PHB-HV/PHB-HP blends, on the other hand, PHB-HV leads to relatively thick lamellas. Since the HP units in the PHB-HP chains cannot participate in the PHB-type lattice, only the homogeneous sequences of HB units longer than the lamellas can participate in the lamellas induced by PHB-HV. Thus, PHB-HP hardly cocrystallize with PHB-HV in PHB-HV/PHB-HP blends. In this manner, the difference in the compatibility of HV and HP units to the PHB crystalline lattice affects the crystallization of the blends of PHB-HV and PHB-HP.

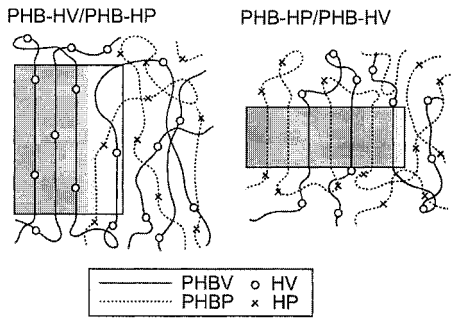

Figure 5. Schematic diagram illustrating the difference in the crystallization process between PHBV/PHBP and PHBP/PHBV blends. Cited from ref.17 and rearranged.

Comparison between PHB-HV and PHB/PHB-HV blends. By the comparison of the solid-state structures and crystallization kinetics between the PHB-HV copolymers with narrow chemical compositional distribution and the PHB/PHB-HV blends of types I and II, the boundary between the PHB/PHB-HV blend that can be regarded as a simple PHB-HV and the one that must be treated as an exact blend are estimated.[11] PHB and HV contents in the cocrystalline phase, crystallinity, lamellar structures, spherulite growth rate and melting behavior were compared. In these data, no difference was observed between the type-I PHB/PHB-HV blends and the PHB-HV copolymers with the same overall HV content. Therefore, we can equate the type-I PHB/PHB-HV blends with PHB-HV copolymers of the same overall HV content. On the other hand, the type-II PHB/PHB-HV blends have amorphous layers thicker than that of the PHB-HV copolymers with the same overall HV content. The difference is, however, not so large and other properties such as melting temperature and spherulite growth rate are similar. Therefore, we can practically regard the type-II blends as a copolymer in some case. Needless to say, the PHB/PHB-HV blends forming more than two crystalline phases (Types III-V) have to be treated as exact blends.

The simplest method to identify the phase structure of PHB/PHB-HV blends and PHB-HV with a broad CCD is to measure the DSC melting curve and to compare the melting

temperature of the blends with PHB-HV copolymers with a narrow CCD. The melting temperature of PHB-HV with a narrow CCD has been reported elsewhere.[2] Immiscible blends and blends forming more than two crystalline phases have two or more melting peaks. The blends forming complete cocrystals have only one melting peak at the temperature expected from the average HV content. If the melting temperature is higher than expected, the crystalline phase rich in the component with a higher crystallization rate is formed.

[1] N. Yoshie, Y. Inoue, *Int. J. Biol. Macromol.*, **1999**, *25*, 193.
[2] N. Yoshie, H. Menju, H. Sato, Y. Inoue, *Macromolecules*, **1995**, *28*, 6516.
[3] A. Cao, M. Ichikawa, K. Kasuya, N. Yoshie, N. Asakawa, Y. Inoue, Y. Doi, H. Abe, *Polym. J.*, **1996**, *28*, 1096.
[4] T. L. Bluhm, G. K. Hamer, R. H. Marchessault, C. A. Fyfe, R. P. Veregin, *Macromolecules*, **1986**, *19*, 2871.
[5] N. Kamiya, M. Sakurai, Y. Inoue, R. Chûjô, Y. Doi, *Macromolecules*, **1991**, *24*, 2178.
[6] N. Yoshie, H. Menju, H. Sato, Y. Inoue, *Polym. J.*, **1996**, *28*, 45.
[7] M. Saito, Y. Inoue, N. Yoshie, *Polymer*, **2001**, *42*, 5573.
[8] S. J. Organ, P. J. Barham, *Polymer*, **1993**, *34*, 459.
[9] S. J. Organ, *Polymer*, **1994**, *35*, 86.
[10] R. P. Pearce, R. H. Marchessault, *Macromolecules*, **1994**, *27*, 3869.
[11] Y. Yoshie, M. Saito, Y. Inoue, *Polymer*, **2004**, *45*, 1903.
[12] N. Kamiya, M. Sakurai, Y. Inoue, R. Chûjô, *Macromolecules*, **1991**, *24*, 3888.
[13] P. A. Barker, P. J. Barham, J. Martinez-Salazar, *Polymer*, **1997**, *38*, 913.
[14] Y. Doi, M. Kunioka, Y. Nakamura, K. Soga, *Macromolecules*, **1987**, *20*, 2988.
[15] N. Yoshie, M. Fujiwara, M. Ohmori, Y. Inoue, *Polymer*, **2001**, *42*, 8557.
[16] N. Yoshie, A. Asaka, K. Yazawa, Y. Kuroda, Y. Inoue, *Polymer*, **2003**, *44*, 7405.
[17] N. Yoshie, A. Asaka, Y. Inoue, *Macromolecules*, **2004**, *37*, 3770.
[18] N. Yoshie, Y. Goto, M. Sakurai, Y. Inoue, R. Chûjô, Y. Doi, *Int. J. Biol. Macromol.*, **1992**, *14*, 81.
[19] S. Bloembergen, D. A. Holden, G. K. Hamer, T. L. Bluhm, R. H. Marchessault, *Macromolecule*, **1986**, *19*, 2865.
[20] H. Bauer, A. J. Owen, *Coll. Polym. Sci.* **1988**, *266*, 241.
[21] M. Scandola, G. Ceccorulli, M. Pozzoli, M. Gazzano, *Macromolecules*, **1992**, *25*, 1405.
[22] M. Kunioka, A. Tamaki, Y. Doi, *Macromolecules*, **1989**, *22*, 694.
[23] N. Yoshie, M. Saito, Y. Inoue, *Macromolecules*, **2001**, *34*, 8953.
[24] H. Abe, Y. Doi, H. Aoki, T. Akehata, *Macromolecules*, **1998**, *31*, 1791.
[25] A. Cao, N. Asakawa, N. Yoshie, Y. Inoue, *Polymer*, **1999**, *40*, 3309.